Supplement of Atmos. Chem. Phys., 22, 10023–10043, 2022
https://doi.org/10.5194/acp-22-10023-2022-supplement

Atmospheric Chemistry and Physics
Open Access

Supplement of

Secondary aerosol formation in marine Arctic environments: a model measurement comparison at Ny-Ålesund

Carlton Xavier et al.

Correspondence to: Carlton Xavier (carlton.xavier@helsinki.fi) and Pontus Roldin (pontus.roldin@nuclear.lu.se)

Supplementary information

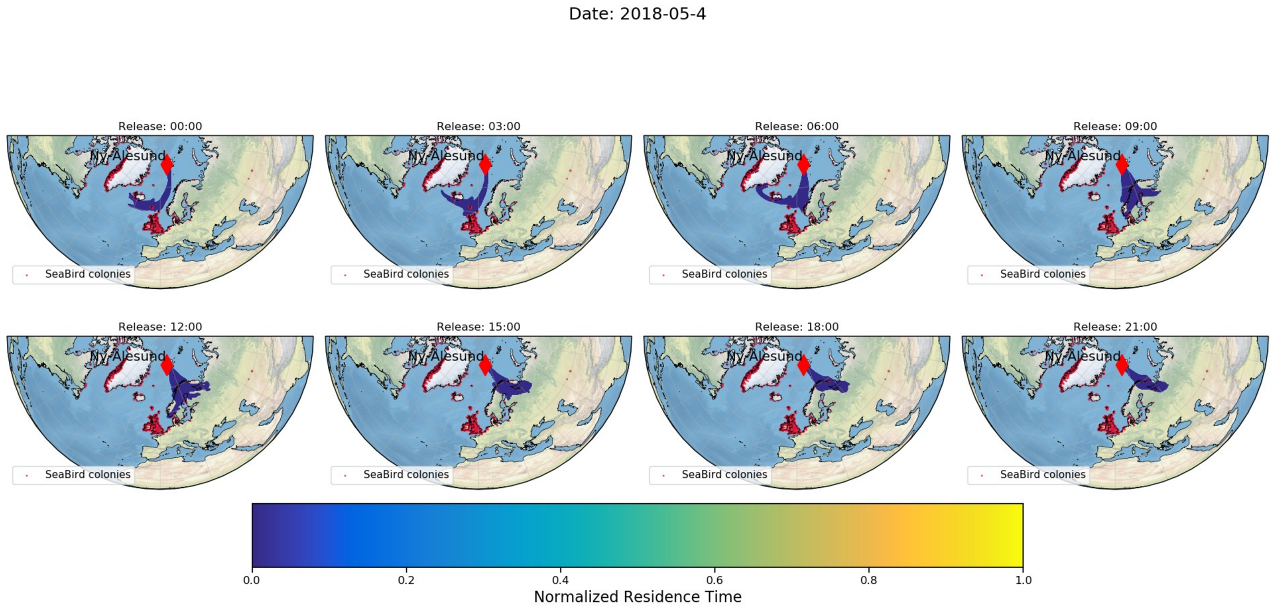

Figure S1: An example plot of normalized potential emission sensitivities (residence time) for 4th May, 2018. There are 8 trajectories per day, arriving every 3 hours (00:00 → 21:00) at Ny-Ålesund. On this particlular day the air amss traverses over the European continent for most of the day. The red points represent the sea bird colonies.

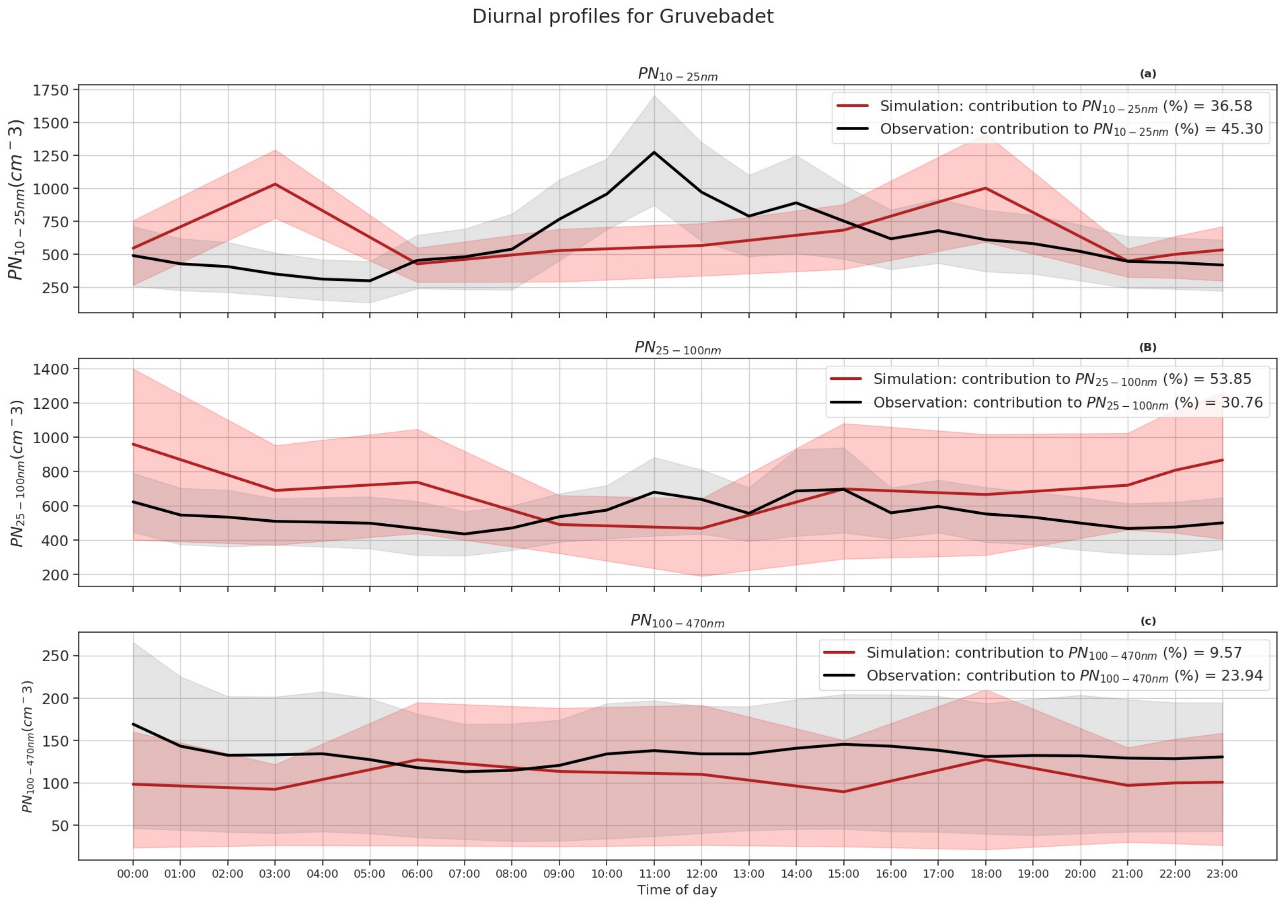

Figure S2: Diurnal profile for Gruvebadet. Panel (a) shows number concentration in nucleation mode $PN_{<25\ nm}$, panel (b) shows number concentration in Aitken mode ($PN_{25-100\ nm}$) and panel (c) shows number concentration in the accumulation mode ($PN_{>100\ nm}$). The red and grey shaded areas represent the 25th and 75th percentile. The legends include the contribution of each mode to the total aerosol number concentration.

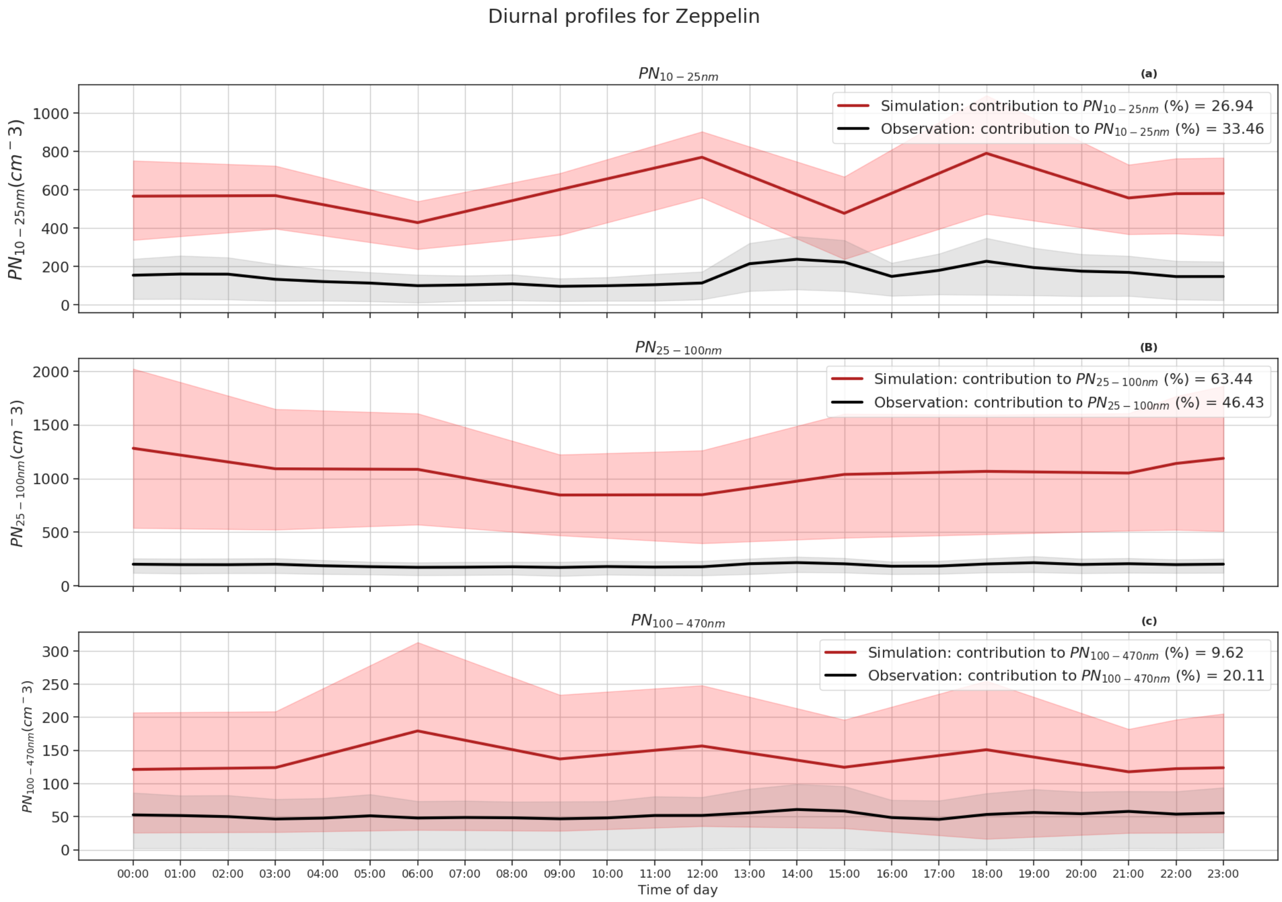

Figure S3: Diurnal profile for Zeppelin. Panel (a) shows number concentration in nucleation mode $PN_{<25\ nm}$, panel (b) shows number concentration in Aitken mode ($PN_{25\text{-}100\ nm}$) and panel (c) shows number concentration in the accumulation mode ($PN_{>100\ nm}$). The red and grey shaded areas represent the 25th and 75th percentile. The legends include the contribution of each mode to the total aerosol number concentration.

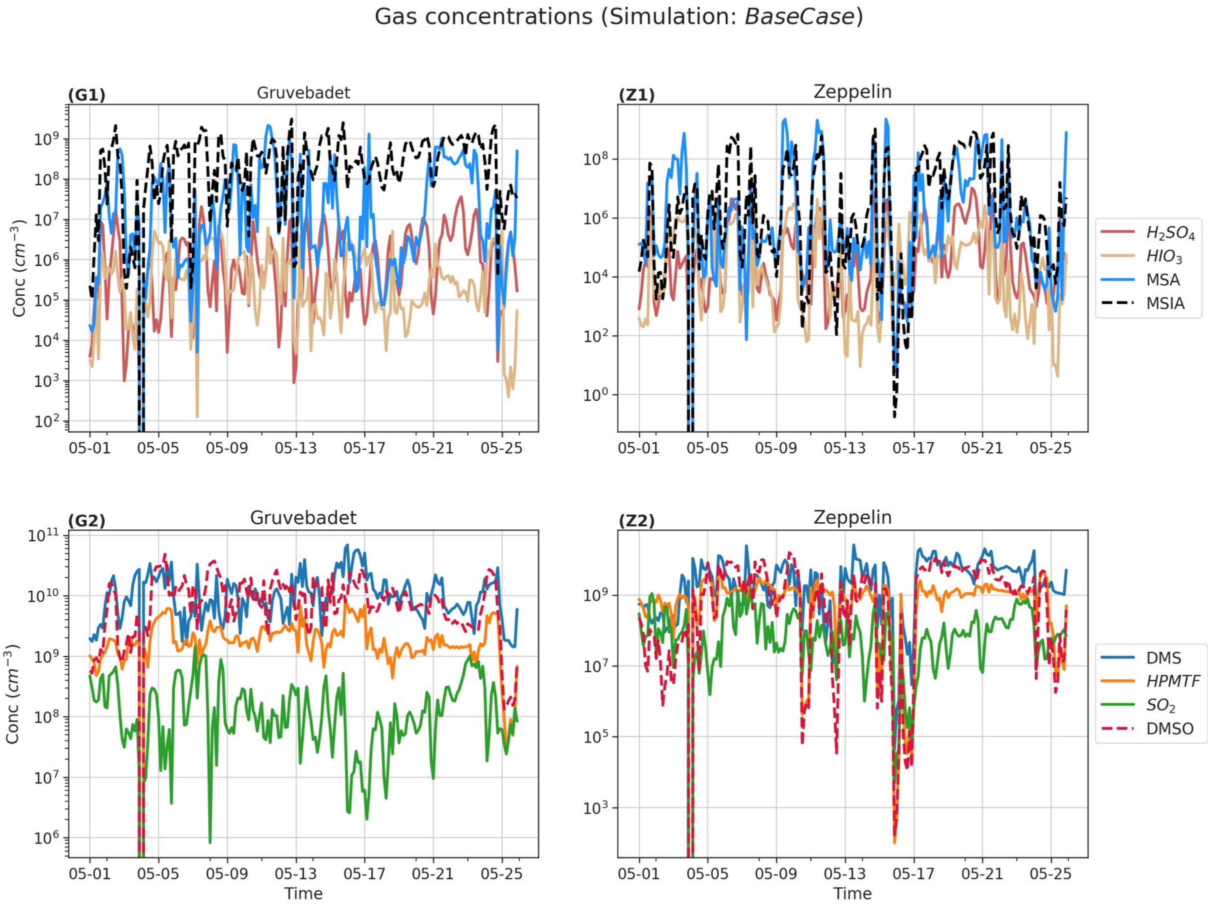

Figure S4. Gas-phase concentrations for the *BaseCase* simulations. The upper two panels **(G1)** and **(Z1)** show the gas-phase concentrations at Gruvebadet and Zeppelin respectively, for compounds H_2SO_4 (red), HIO_3 (gold), MSA (cyan), MSIA (dotted black) and the lower panels **(G2)** and **(Z2)** show the gas-phase concentrations for DMS (blue), HPMTF (orange), SO_2 (green) and DMSO (dotted red). Note the different ordinate scales.

The SO_2 gas-phase concentrations are in the order of 10^6-10^9 # cm^{-3} (with monthly mean values 1.7 x 10^8 # cm^{-3}), which is a factor of 2.3 higher than the average concentrations measured for spring 7.6 x10^7 # cm^{-3} by (Lee et al., 2020) at Zeppelin (Figure S4). The monthly mean simulated H_2SO_4 gas phase concentrations (6.8 x 10^5 # cm^{-3}) also agree well with the estimated H_2SO_4 proxy (Eq. S1, supplementary) spring average values of 7.5 x 10^5 # cm^{-3} (Lee et al., 2020) at Zeppelin

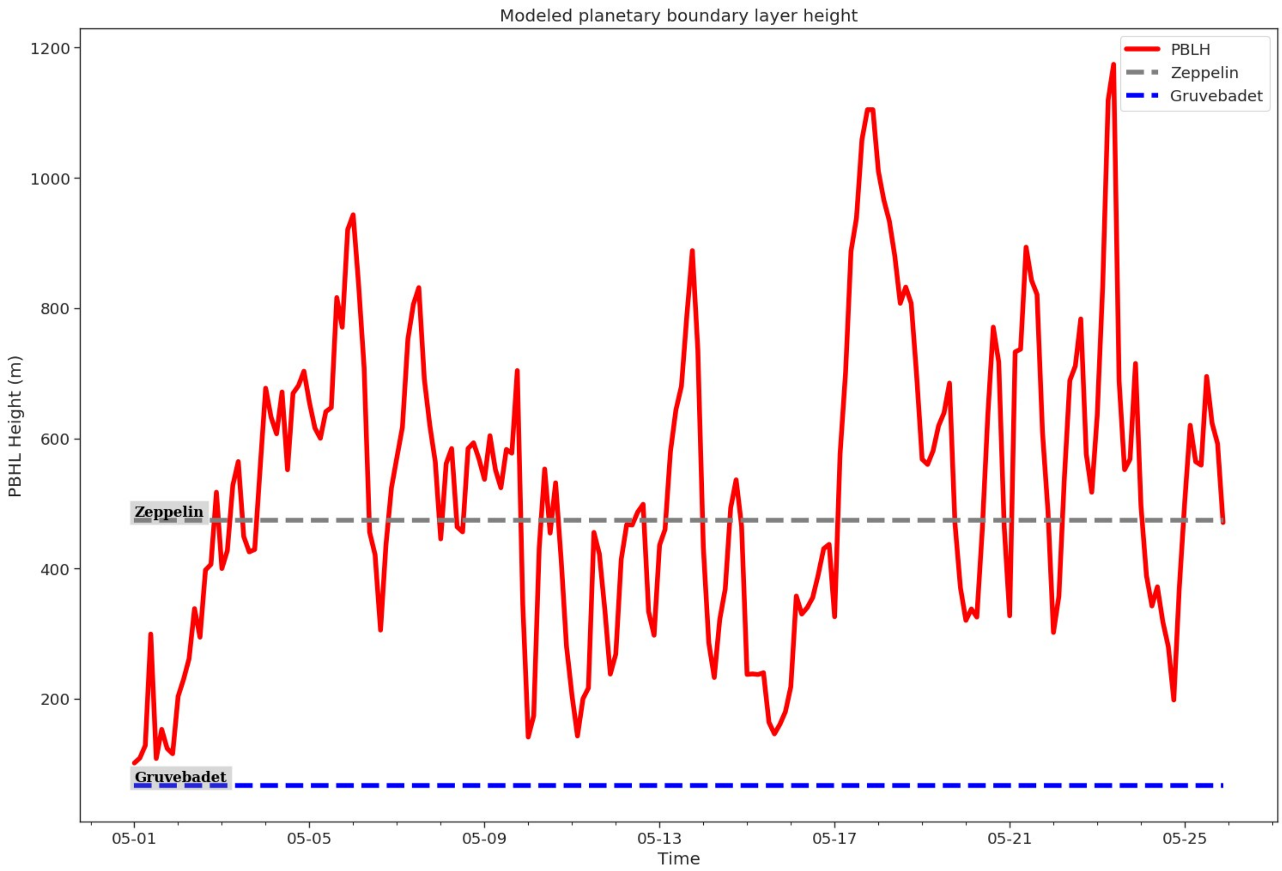

Figure S5: Modeled Planetary boundary layer height (PBHL) for the entire selected period. The grey dashed line marks Zeppelin station, while the blue dashed line marks Gruvebadet measurement station. The PBHL was modeled using Flexpartv10.4.

Modeled proxy H2SO4 concentrations

The modeled gas phase H_2SO_4 concentrations was compared to the mean spring gas H_2SO_4 concentrations derieved by (Lee et al., 2020) for the period between October 2016 and Decemmber 2018. Eq S1 shows the empirical proxy model of H_2SO_4:

$[H_2SO_4] = a \,.\, k \,.\, [SO_2]^b .\ SRAD^c .\ (CS.RH)^d$ (Eq. S1)

where $[SO_2]$ is the gas phase SO^2 concentrations (molecules cm^{-3}), SRAD is the solar radiation (W m^{-2}), CS is the condensation sink (s^{-1}) and RH is the relative humidity. '*k'* is the ambient temperature-dependent reaction rate constant and constant a=8.21 x 10^{-3}, b= 0.62, c=1 and d= – 0.13 (Lee et al., 2020).

Table S1: The table shows simulated fractional contribution of different compounds to total PM in different size regimes of nucleation (total $PM_{<25nm}$) , Aitken (total $PM_{25-100\ nm}$) and accumulation - coarse (total $PM_{>100nm}$) mode. These values represent the fractional contribution for the *BaseCase* simulation.

Species	**Total nucleation mode PM fraction ($PM_{<25nm}$) (%)**	**Total Aitken mode PM fraction ($PM_{25-100\ nm}$) (%)**	**Total accumulation mode PM fraction ($PM_{100\ nm-1\ \mu m}$) (%)**	**Total coarse mode PM fraction ($PM_{>1\ \mu m}$) (%)**	**Total PM_{10} fractional contribution (%)**
SO_4^{2-}	73.99	71.00	5.96	3.36	6.67
NH_4^+	12.34	6.95	0.13	0.06	0.21
Cl^-	2.36	1.98	39.96	43.36	39.54
Na^+	8.02	11.92	32.90	34.17	32.91
MSA	3.26	8.12	20.58	18.85	20.45
HIO_3	0.004	0.004	0.05	0.05	0.05
NO_3^-	0.006	0.01	0.17	0.15	0.17

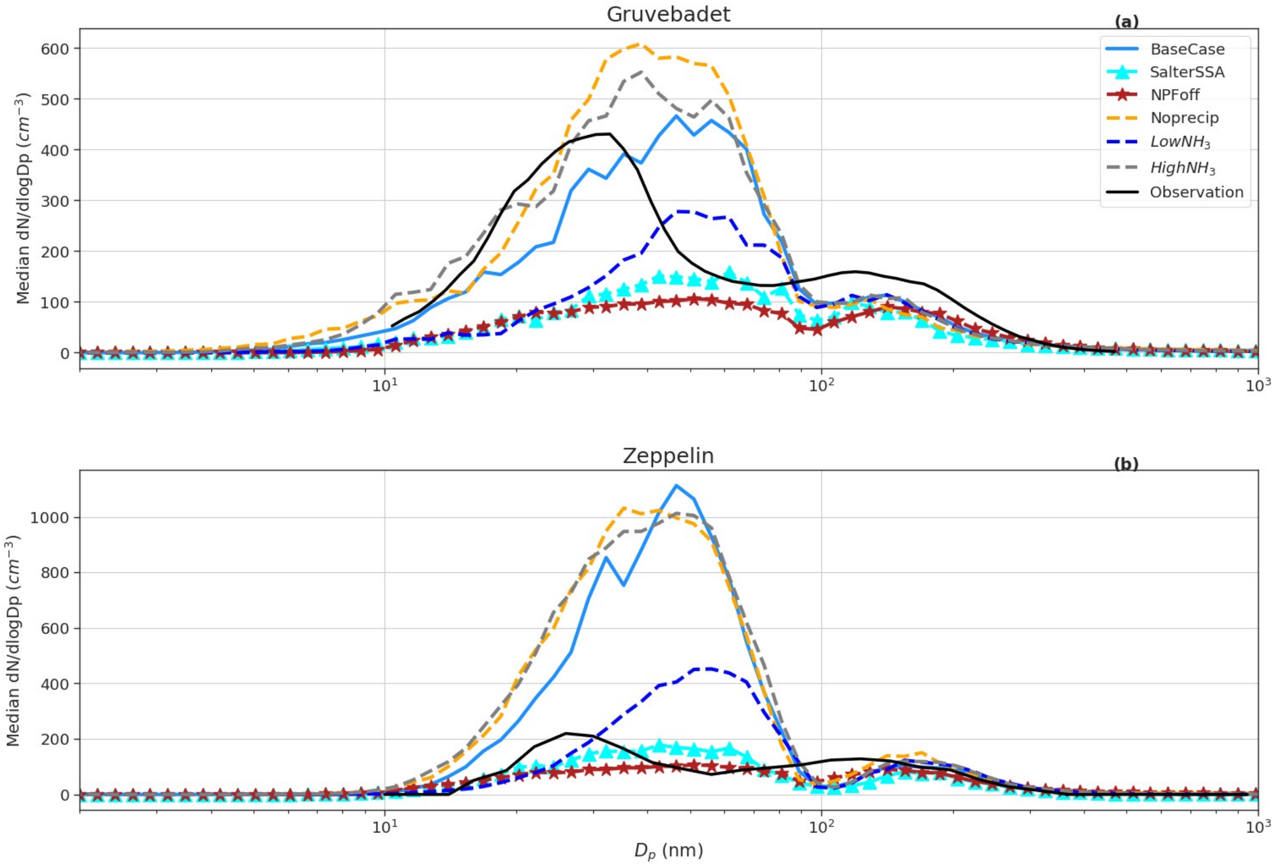

Figure S6: Median particle size distribution for sensitivity cases including *BaseCase* and observations for both stations Gruvebadet (panel (a)) and Zeppelin (panel (b)).

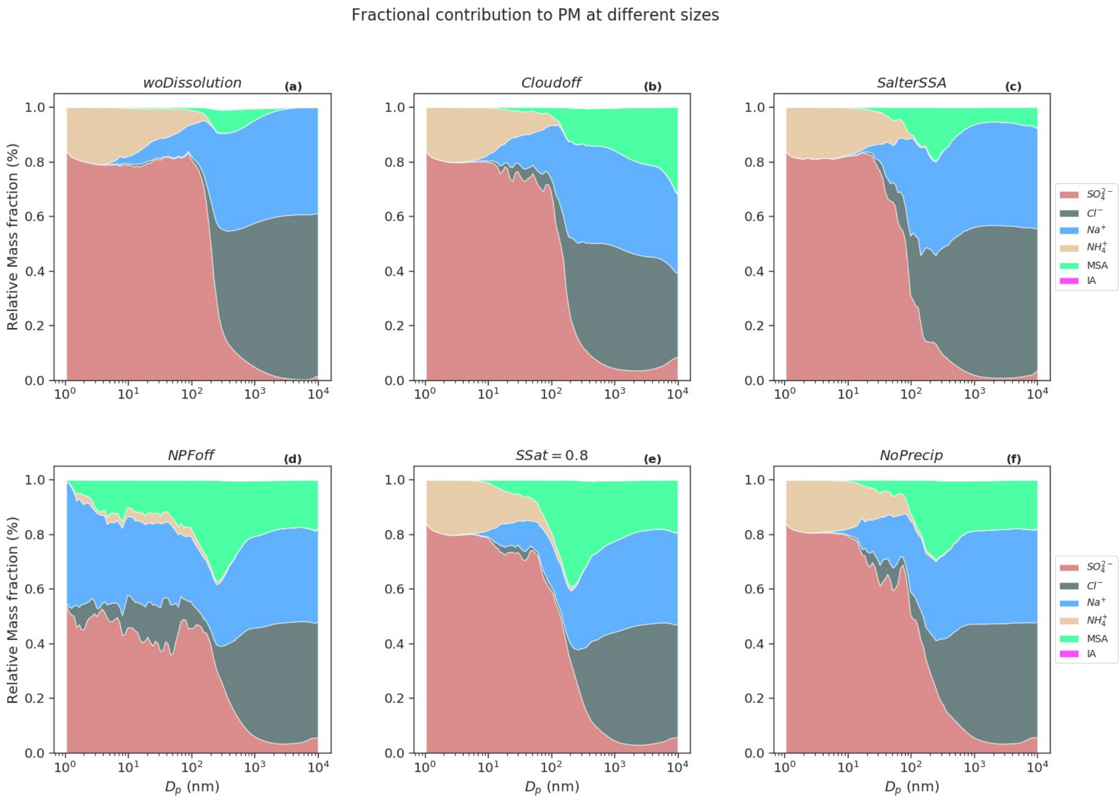

Figure S7: Fractional contribution to PM by different constituent compounds for different sensitivity tests.

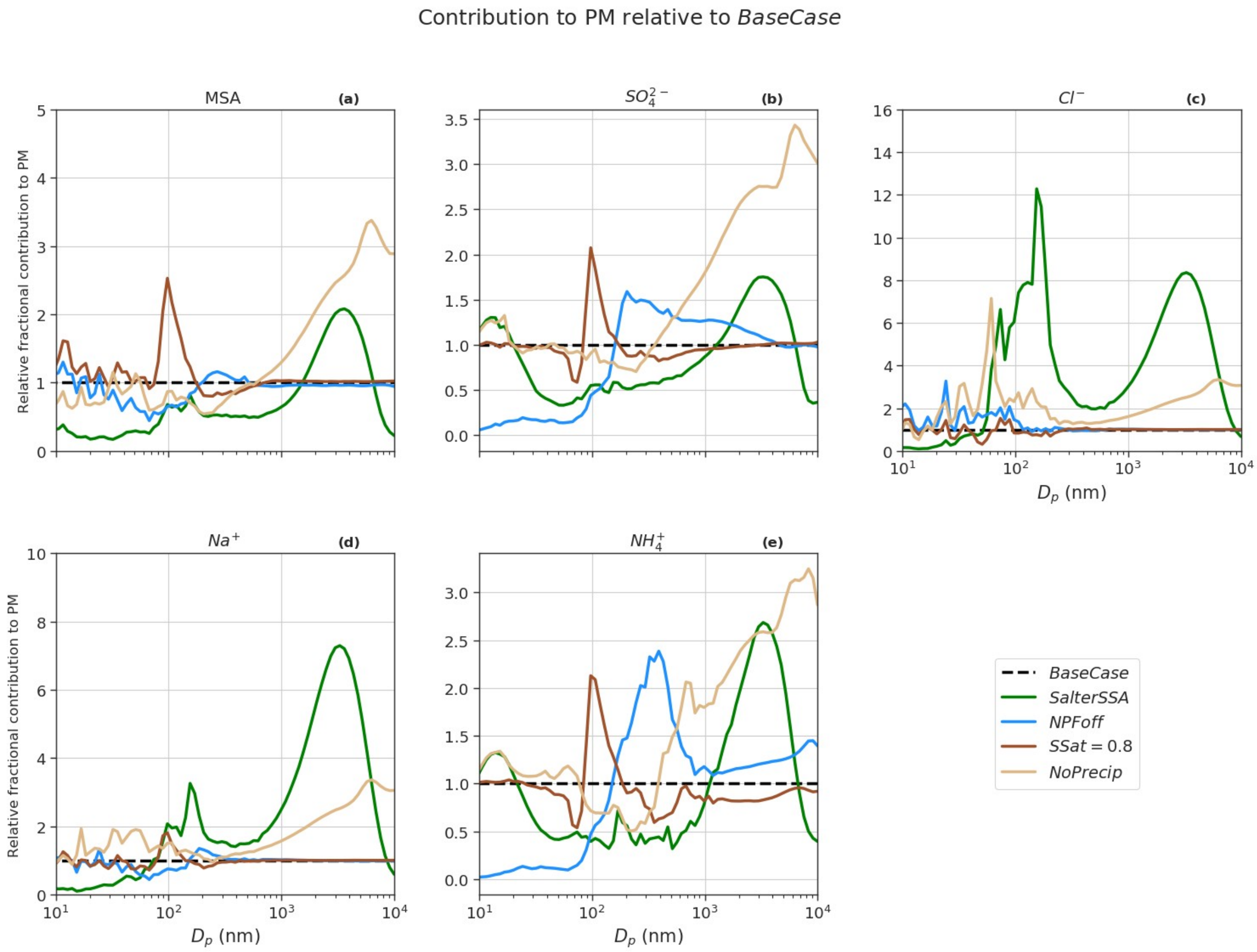

Figure S8: Contribution of constituent compounds, namely, MSA (panel (a)), SO_4^{2-} (panel (b)), Cl^- (panel(c)), Na^+ (panel (d)) and NH_4^+ (panel (e)) to PM with respect to *BaseCase* (the black dotted line).

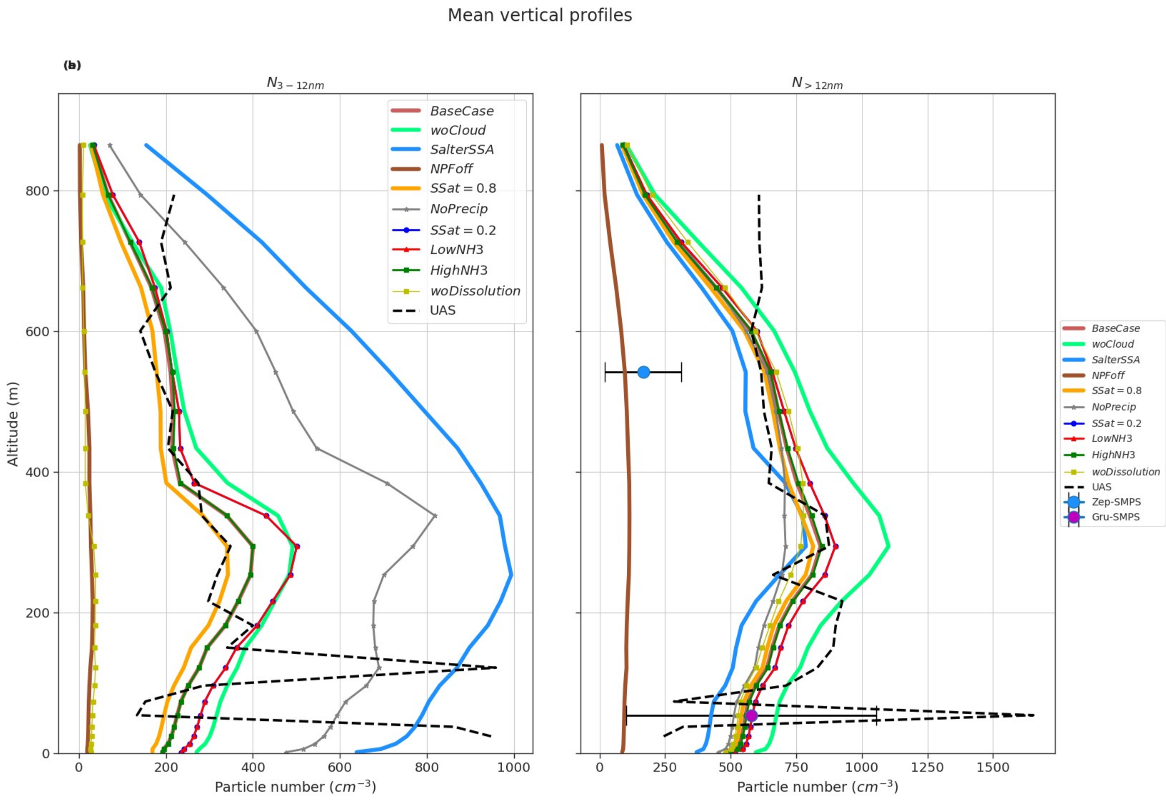

Figure S9: Mean vertical number concentration profiles for $N_{3\text{-}12\text{ nm}}$ (panel (a)) and $N_{>12\text{ nm}}$ (panel (b)) for different cases compared to the measured vertical profile (black dashed line) and average Zepplein and Gruvebadet SMPS data. The large variation in the vertical profiles further serve to underline the influence of various uncertain parameters associated with marine air-masses (such as cloud supersaturations, NH_3 concentrations) on particle concentrations and their vertical profiles.

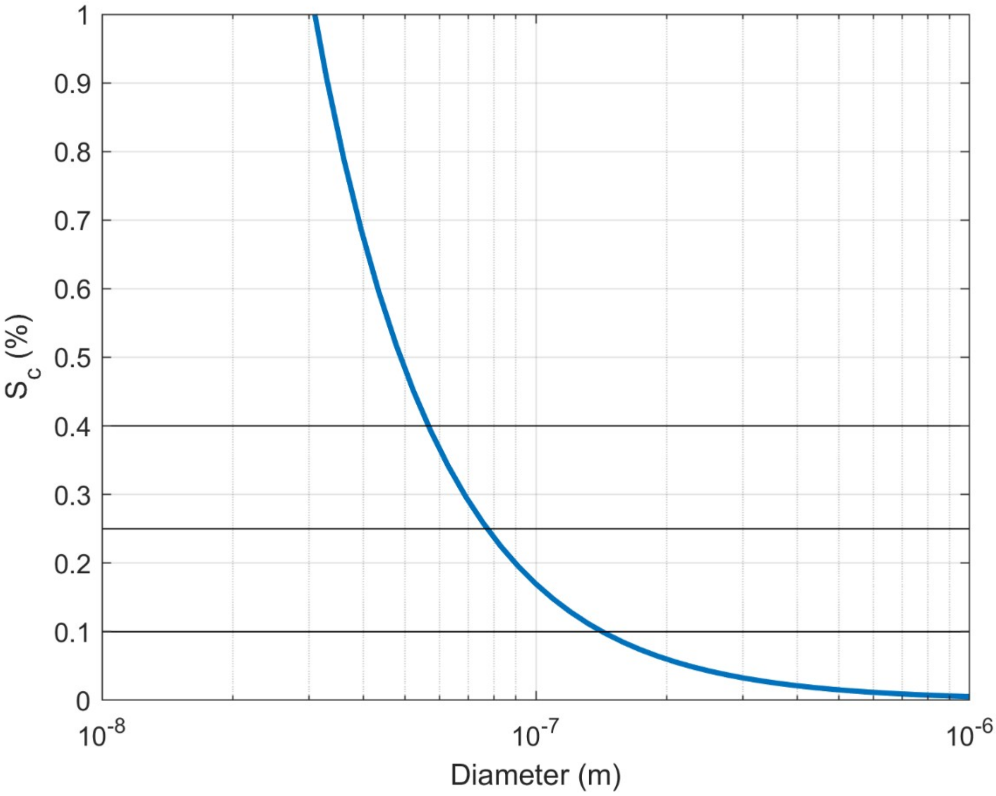

Figure S10: Calculated water vapor supersaturation above the particle surface (*S_c*) for pure ammonium sulfate particles at 273.15 K. The cloud supersaturation (*S*) of 0.1%, 0.25% and 0.4% used in the different ADCHEM model simulations are illustrated by the bold black horizontal lines.

References

Lee, H., Lee, K., Lunder, C. R., Krejci, R., Aas, W., Park, J., Park, K.-T., Lee, B. Y., Yoon, Y. J. and Park, K.: Atmospheric new particle formation characteristics in the Arctic as measured at Mount Zeppelin, Svalbard, from 2016 to 2018, Atmos. Chem. Phys., 20(21), 13425–13441, doi:10.5194/acp-20-13425-2020, 2020.